ISME

Simulating Cooling Injection Effect of Trailing Edge of Gas Turbine Blade on Surface Mach Number Distribution of Blade

M. Mahmoodi*
Assistant Professor

J. Pirkandi†
Assistant Professor

K. Khoramdel‡
MSc Student

In this research, a gas turbine blade cascade was investigated. Flow analysis around the blade was conducted using RSM and RNG.K-ε turbulence modeling and it is simulated by Fluent software. The results were considered for the cases as Mach number loss at the trailing edge of blade caused by vortexes that were generated at the end of blade. Effect of cooling flow through the trailing edge on the Mach number distribution was also studied at the blade surface. Present results using RSM and RNG. K-ε turbulence modeling showed that the agreement was good and the capability of the applied model was strong enough to analyze such a complicated flow behavior. According to results from the Mach number distribution on the blade surface, air injection reduces the flow loss at the trailing edge. Comparison of the results shows that air injection at a rate of 3 percent of inlet total air to blade row make changes location of shock on the surface of blade and the loss in turbine blade decreases about 0.7%.

Keyword: Gas turbine blade, Trailing edge, Cooling effect, Cascade, RNG.K-ε and RSM turbulence models

1 Introduction

The investigations conducted in the recent 60 years have supported the increased efficiency of gas turbines. Results of these studies are new methods that increase the efficiency without fundamentally changing the gas turbine. Two of the presented methods have maximum effect on the efficiency increment of gas turbines. The first one is the increase of the gas inlet temperature to turbine that ends in thermal efficiency increase of the gas-turbine cycle. The second one is the design of the gas turbine parts by the application of advanced methods, decreases the loss of energy in different parts or sections.

One of the parts that could have an optimized design in order to noticeably increase the gas turbine's efficiency is the blade profile. In general, turbine blades can be designed by the direct method or reverse method. In the direct method, the designer designs a blade and then its profile is considered by flow analysis in order to estimate the blade behavior. This

---

*Corresponding Author, Assistant Professor, Department of Aerospace, Maleke Ashtar University of Technology, Tehran, mostafamahmoodi@engineer.com
†Assistant Professor, Department of Aerospace, Maleke Ashtar University of Technology, Tehran, j_pirkandi@yahoo.com
‡MSc Student, Department of Aerospace, Maleke Ashtar University of Technology, Tehran, kamrankh2011@yahoo.com

procedure is continued until the blade with an optimized geometry is obtained. Dunham [1] and Pritchard [2] have used this method in their studies. In the reversed method, the designer starts with an initial configuration with an acceptable behavior. Then, improvement is obtained by modification. The output is a new configuration of the blade and its behavior is more suitable and close to the optimized condition. Leonard et al. [3] proposed a procedure for the reverse method to design a turbine blade row and a compressor blade considering all the mechanical and geometrical aspects.

The mentioned both methods are not new and based on flow stability (informality) at the inlet and the outlet, in order to apply the final possible modification. The resulted blade profile with the best trailing edge must be examined in the real flow field with similar conditions and without the designing method.

Numerous works have been done on the flow field around a gas turbine blade during in the last thirty years. According to these works, the experimental and numerical methods can be applied in order to analyze the flow field in Turbomachinery. The two-dimensional flow of a turbine blade can be simulated by a flow inside a single blade row (a row of blades with similar shapes and constant distances at blade length). The condition used to obtain the results from the theoretical and experimental cases must be similar. In other words, the parameters like Mach number, Reynolds number, turbulence, periodical condition from one blade to another, and the boundary layer's thickness must be the same. Verification of the experimental results from a single row blade seems to be difficult and is dominated by parameters like adjustment and calibration of measuring equipment, effect of the surrounding blades, inlet flow development, wall effect, and technical complexity.

In order to analyze the flow field around a single row blade, especially near the blade trailing edge, it is not possible to use the precise measurement equipment because of technological complexity. In this case, the computational fluid dynamics is the best method for estimating flow behavior.

At the beginning, because of the capability limitation of the computers, inviscid flow methods were mostly conducted. One of the successful inviscid methods based on the finite volume is time marching solution of the time dependent Euler equation, which was conducted by Denton [4] for two-dimensional methods. In this method, velocity and pressure field can be predicted properly at far distance from wall. However, analysis of complex flow because of viscosity needs to solve full Navier-Stokes equations around a blade, which is difficult, especially for turbulent flows.

In the development of any modern aero engine, the most expensive component is the high-pressure turbine due to the harsh environment (high temperatures downstream of the combustor and mechanical solicitations) [5]. Higher loading per row allows to reduce the number of stages, limiting the weight of the machine. It contributes therefore to lower the fuel consumption of commercial aircrafts. However, an increase of load implies that the flow across the turbine passages is transonic, resulting in shock-wave interactions.

In general, high-temperature gas passes through a turbine cascade and thus they use a certain type cooling [6]. The cooling flow can be injected through the holes in the blade. Thus, the cooling flow will affect the mainstream flow [7]. The internal fluid mechanic losses for a turbine blade with trailing edge coolant ejection was Investigated by Uzol et al. [8]. Their study was a detailed experimental investigation of the external subsonic flow field near the trailing edge and the investigation of the external aerodynamic loss characteristics of the turbine blade with trailing edge coolant ejection system [9]. Their results showed that the aerodynamic penalty levels in the wake region near the trailing edge are increased due to the mixing of the coolant and mainstream flows for 0–3 percent ejection rates.

Horbach et al. [10] was concentrated on trailing edge film-cooling of modern high-pressure turbine blades using coolant ejection through planar slots with a pressure side cutback. The effects of different geometric configurations on the structure and the performance of the cooling-film was investigated in terms of film-cooling effectiveness, heat transfer coefficients, and discharge behavior.

Finally, aerodynamic losses in turbines with and without film Cooling, as Influenced by mainstream turbulent, surface roughness, airfoil Shape, and Mach number were investigated by Phil Ligrani [11]. They described the influences of a variety of different physical phenomena as they affect the aerodynamic performance of turbine airfoils in compressible, high-speed flows with either subsonic and transonic Mach number distributions.

2 Governing equations

The governing equations for a single-phase flow contain the conservation of mass, momentum or Navier-Stokes, and energy equations [12].

$$\frac{\partial}{\partial t}(\rho\phi) + \mathrm{div}(\rho\vec{u}\phi) = \mathrm{div}(\Gamma \mathrm{grad}\phi) + s \tag{1}$$

Transient term, convection term, diffusion term, and source term of Eq. (1) are the basis for the differentiation of the numerical solution. In the Navier-Stokes equation, shear stress can be modeled with respect to flow regime (laminar or turbulence) and Reynolds number as:

$$\tau_{ij} = \mu\left(\frac{\partial u_i}{\partial x_j} + \frac{\partial u_j}{\partial x_i}\right) - \frac{2}{3}\mu\frac{\partial u_l}{\partial x_l}\delta_{ij} \tag{2}$$

Modeling is possible and can be simple when flow is laminar. However, an advanced modeling should be used for the turbulence flow regimes. In the present attempt, two turbulence models of RNG.K-ε and RSM were used for the turbulence flow modeling.

3 Solution of the equations using RNG.K-ε turbulence model

Models with two equations have been the basis of turbulence flow research during the last three decades. These models not only use an equation for estimating k (kinetic energy of flow fluctuation per mass unit), but also apply an equation for estimating the longitudinal scale of turbulence flow. Therefore, the models with two equations are generally a complete model. This means that they can be used for the estimation of a turbulence flow character without having the knowledge from the past history of that flow. One of the frequent uses of the models with two equations for turbulent flow is K-ε model. It is used in two forms of K-ε standard and RNG-K-ε model.

The main weakness for the K-ε standard model is that this model over-predicts the turbulence kinetic generation rate, which causes an error during the estimation of turbulence viscosity and the related stresses. The over-prediction of the turbulence energy is transferred to the downstream of the flow that results in unreal estimated results and flow separation. In this research, RNG.K-ε turbulence model was used to solve the flow field equations.

The mentioned model is a two-equation model that is obtained by mathematical methods and is derived from the conservation equations that govern the flow field. Therefore, the coefficient that is used in this model is not obtained from an experiment, but has a mathematical basis that predicts the separation zone and wakes with higher accuracy[13&14]. The two equations are as:

$$\rho\frac{DK}{Dt} = \frac{\partial}{\partial x_i}\left(\alpha_k\mu_{eff}\frac{\partial k}{\partial x_i}\right) + G_K + G_b - \rho\varepsilon - Y_M \tag{3}$$

$$\rho\frac{D\varepsilon}{Dt}=\frac{\partial}{\partial x_i}\left(\alpha_\varepsilon\mu_{eff}\frac{\partial\varepsilon}{\partial x_i}\right)+C_{1\varepsilon}\frac{\varepsilon}{k}(G_K+C_{3\varepsilon}G_b)-C_{2\varepsilon}\rho\frac{\varepsilon^2}{k}-R \tag{4}$$

where G_K is turbulence kinetic energy generation due to mean velocity fluctuation (variation),G_b is kinetic energy generation due to buoyancy, Y_M is variation of expansion in the compressible turbulence due to the loss rate that is estimated in the turbulence model by the compressibility effect, and a_k and a_ε are effects of Prandtl reverse for K and ε, respectively. The turbulence viscosity can be obtained from the following equation:

$$\mu_t=\rho c_\mu\frac{k^2}{\varepsilon} \tag{5}$$

R is obtained from the following equation:

$$R=\frac{c_\mu\rho\eta^3(1-\frac{\eta}{\eta_0})\varepsilon^2}{(1+\beta\eta^3)k} \tag{6}$$

Where

$$\eta=\frac{sk}{\varepsilon}\ \ ,\eta_0=4.38\ ,\beta=0.012 \tag{7}$$

$$s=\sqrt{2s_{ij}s_{ij}}\ ,\ \ s_{ij}=\frac{1}{2}\left(\frac{\partial u_i}{\partial x_j}+\frac{\partial u_j}{\partial x_i}\right) \tag{8}$$

$$C_{2\varepsilon}=\tanh\left|\frac{\upsilon}{u}\right| \tag{9}$$

where v is the velocity component parallel to the gravity and u is the flow velocity component normal to the gravity field constant values in RNG.K-ε model are defined as $c_\mu=0.0845$, $C_{2\varepsilon}=1.68$, $C_{1\varepsilon}=1.42$.

The boundary conditions for k and ε are obtained using the following equations:

$$k=\frac{3}{2}(u_{ave}I)^2 \tag{10}$$

Where $u_{ave}$is mean flow velocity and I is turbulence intensity.

$$\varepsilon=c_\mu^{\frac{4}{3}}\frac{K^{\frac{3}{2}}}{l} \tag{11}$$

c_μ is an experiment constant equal to $c_\mu=0.09$, l is flow length scale that, using the following equation for the flow developed in ducts, is calculated as l = 0.07L, and L is hydraulic diameter of the inlet duct as L = D_H. Hydraulic diameter is equal to the distance between the turbine blades (pitch). Thus, k and ε can be calculated with hydraulic diameter and turbulence intensity. Turbulence intensity is usually in the range of 1 to 10% of the average kinetic energy.

4 Solution of the equations using RSM turbulence modeling

The Reynolds stress equations model is one of the best estimate models for solving the turbulence flow field. The RSM model is obtained from the Navier-Stokes equations accompanying an equation for estimating the losses. The turbulence RSM model estimates more accurate results for complicated flows than the models with one and two equations models [15].

$$\frac{DR_{ij}}{Dt}=P_{ij}+D_{ij}-\varepsilon_{ij}+\Pi_{ij}+\Omega_{ij} \tag{12}$$

The above terms in the equations must be modeled by the assumption equation where $R_{ij}=\overline{u'_i u'_j}$ is rate of change, P_{ij} is rate of production, D_{ij} is transport by diffusion, ε_{ij} is rate of dissipation, Π_{ij} is transport due to turbulent pressure-strain interactions, and Ω_{ij} is transport due to rotation. ω_k is rotation vector and e_{ijk} is -1, 0, or 1 depending on the indices.

$$P_{ij} = -\left(R_{im}\frac{\partial U_j}{\partial x_m} + R_{jm}\frac{\partial U_i}{\partial x_m}\right) \tag{13}$$

$$D_{ij} = \frac{\partial}{\partial x_k}\left(\overline{u'_i u'_j u'_k} + \overline{p'\left(\delta_{jk} u'_i + \delta_{ik} u'_j\right)}\right) \tag{14}$$

$$\varepsilon_{ij} = 2\mu\overline{\frac{\partial u'_i}{\partial x_k}\frac{\partial u'_j}{\partial x_k}} \tag{15}$$

$$\Pi_{ij} = -p'\left(\frac{\partial u'_i}{\partial x_j} + \frac{\partial u'_j}{\partial x_i}\right) \tag{16}$$

$$\Omega_{ij} = -2\omega_k\left(R_{jm}e_{ikm} + R_{im}e_{jkm}\right) \tag{17}$$

5 Results

For modeling and flow analysis, a Brite 22 N type blade profile was selected (Figure (1)) and Fluent software is used. The trailing edge shape was curved. The curved type is called TE (trailing edge blade) and has precise and accurate geometry. The operational conditions were defined properly as presented in Table (1). The flow analysis was conducted for two-dimensional models with and without the cooling air injection through the trailing edge.

Width of slot at the trailing edge for outlet cooling air was approximately 0.3 times of the trailing edge thickness. A parameter called mass flow coefficient, C_m, was defined as the amount of the cooling air outlet from the trailing edge slot to the total amount of the air inlet to a single row blade. The total inlet pressure and outlet static pressure were used as the boundary conditions. The blade was assumed to be in adiabatic conditions. The boundaries for the blades were periodic in order to similarly model the single row blades. To facilitate the modeling and analysis of blade rows, blade profile was divided into two parts of pressure side and the suction (Figure (2)). Modeling including inlet and outlet boundaries a according to the outlet angle of 73 degrees, the periodic boundaries of the flow upstream was drawn with angle of 73 degrees. For the numerical solution of the governing equations by control volume method, the whole space was divided into small control volumes.

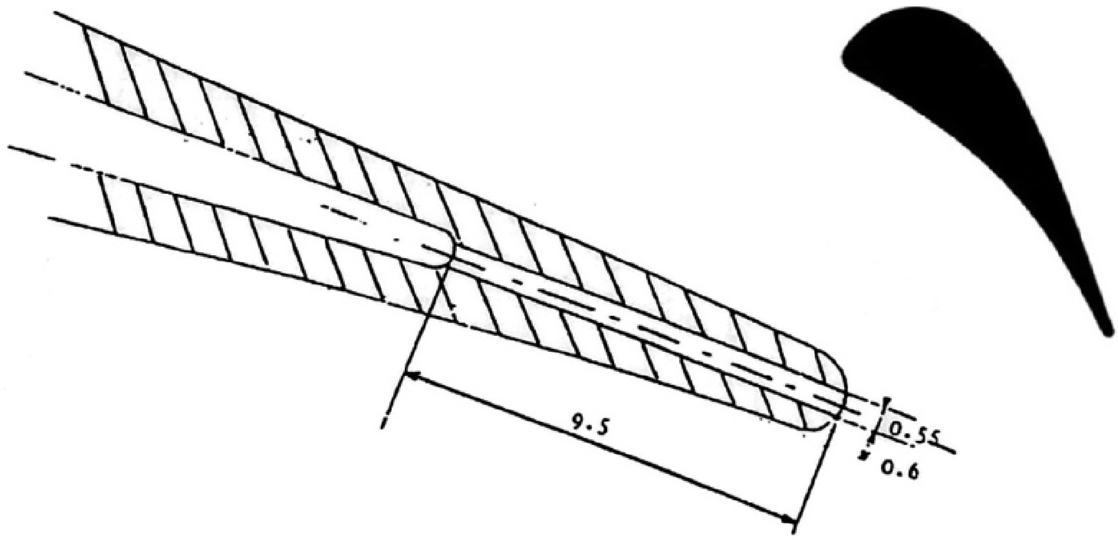

Figure 1 Brite 22 N type blade profile that is called TE type with air injection slot configuration

All the main and coupling equations were taken into account and solved for each of the control volumes. The type mesh was of H type that coincided with the physics and flow direction. The distance between the meshes changed with respect to the zones which had higher variation. The problem was primarily solved in the coarse meshes and then the grid became finer. Finally, the solution was repeated. Figure (2) shows the geometry and main characteristics of the blade and cascade.

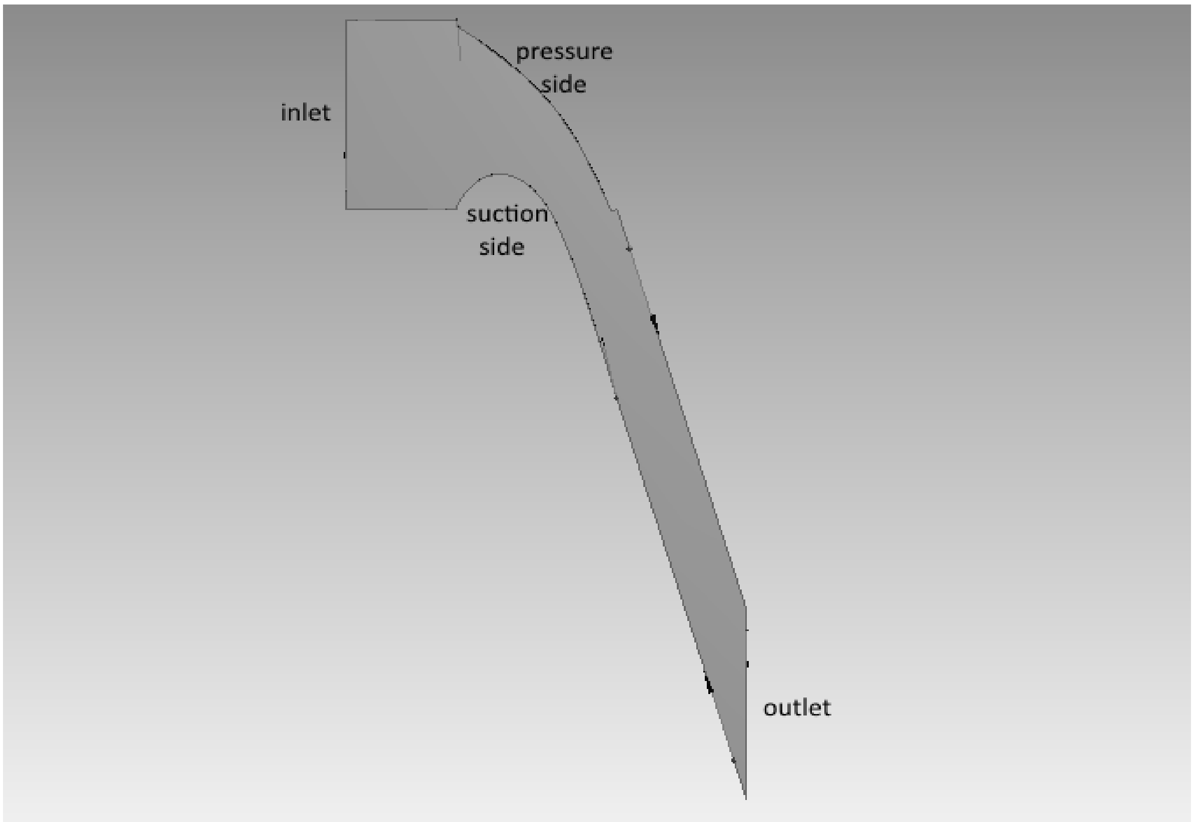

Figure 2 TE type blade of 2D modeling divided to pressure and suction side

Table 1 The Dunker blade specification and wind tunnel

	Symbol	Value
chord length	C	72mm
axial chord length	c_{ax}	43.1mm
pitch to cord ratio	g/c	0.7506
pitch	g	54mm
gauging angle(arccos)	o/g	73.9^o
throat width	o	14.98mm
stagger angle	γ	51.9^o
trailing edge thickness	t_e	1.70mm
trailing edge thickness to chord ratio	t_e/c	2.36%
trailing edge wedge angle	δte	6.4^0
rear suction side turning angle	ε_{ss}	8.2^0
Wind tunnel temperature	T	273k
Turbulence intensity of wind tunnel	t_e	2%

The results obtained from the behavior of blades can be considered qualitatively and quantitatively. In the quantitatively analysis of the row blades, the energy loss value must be estimated. If the qualitative analysis is required, the flow pattern and general behavior are analyzed. At the end, the pressure field distribution and Mach surface are presented. It should be mentioned that the form or boundary layer depend on the distribution of surface Mach number. Along the walls the standard logarithmic wall function y +> 30 is used (Figure (3)). In this way, it can be used near the wall of the larger networks, and consequently will be less computation time.

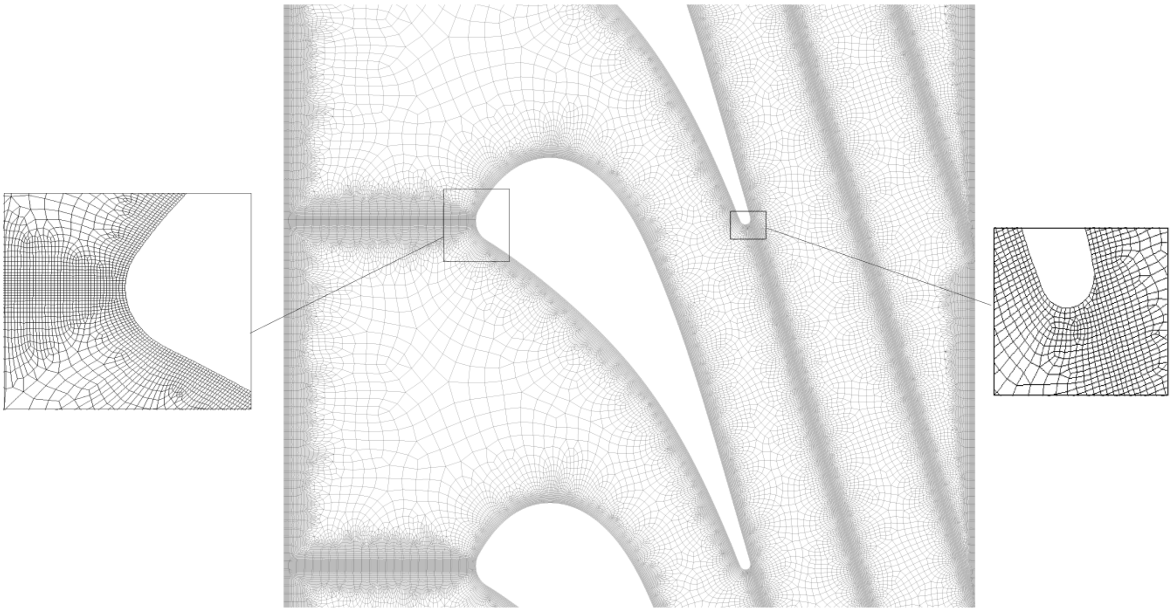

Figure 3 TE type blade periodic grid

Figures (5), (6) and (7) present the surface Mach number distribution for TE blade without cooling air (C_m = 0%) for the outlet isentropic Mach numbers of 0.8, 1.05, and 1.2 using RNG.K-ε turbulence model. In the figures, RSM model was included in addition to RNG.K-ε model. The blade was studied at the flow field with the outlet isentropic Mach numbers of 0.8, 1.05, and 1.2.

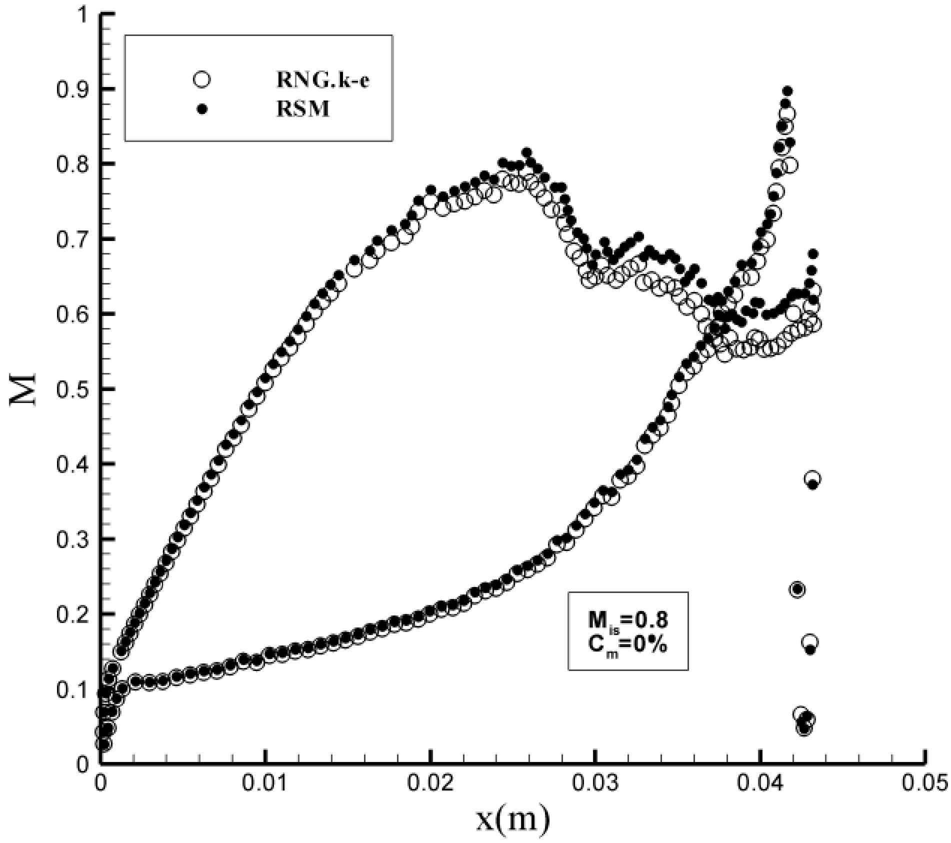

Figure 5 The Mach number distribution on the TE blades without cooling air (C_m = 0%) at Mach 0.8 using turbulence modeling of RNG.k-ε and RSM

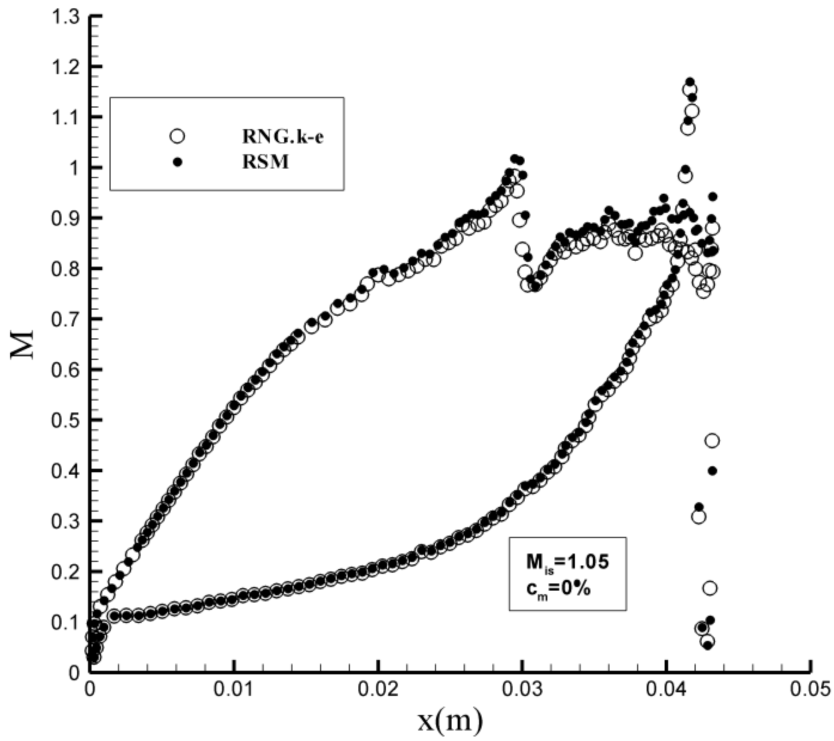

Figure 6 The Mach number distribution on the TE blades without cooling air (C_m = 0%) at Mach 1.05 using turbulence modeling of RNG.k-ε and RSM

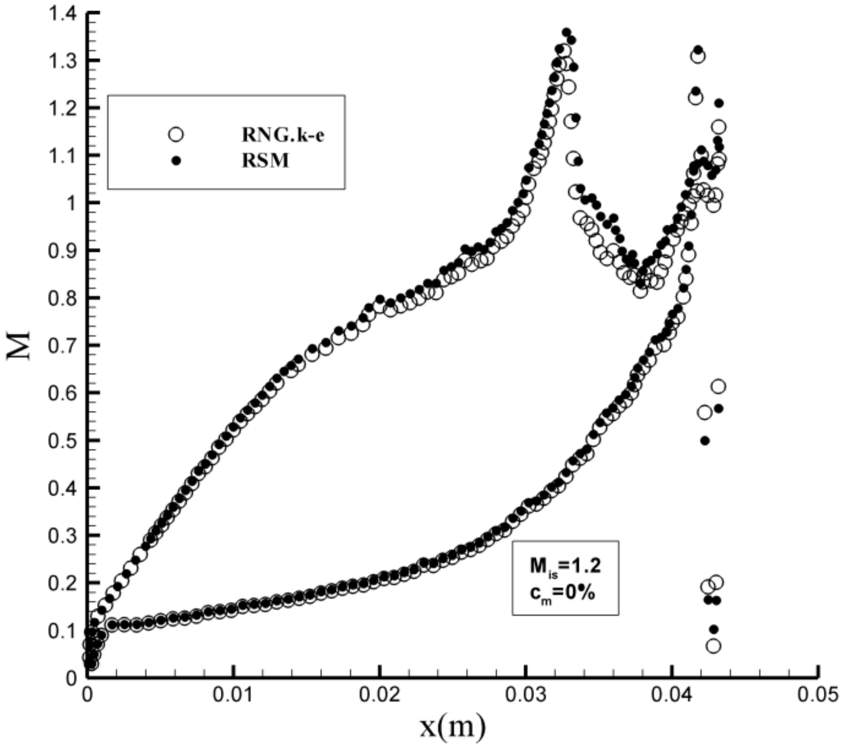

Figure 7 The Mach number distribution on the TE blades without cooling air (C_m = 0%) at Mach 1.2 using turbulence modeling of RNG.k-ε and RSM

Severe loss of the Mach number occurred on the trailing edge of TE blades because of trailing edge curvature. In fact, passing from the surface of the blade created vortices at the end of the trailing edges and the trailing edge at the TS blade caused the Mach number to be decreased at 1.2, which was the effect of the trailing edge shape on the upstream flow.

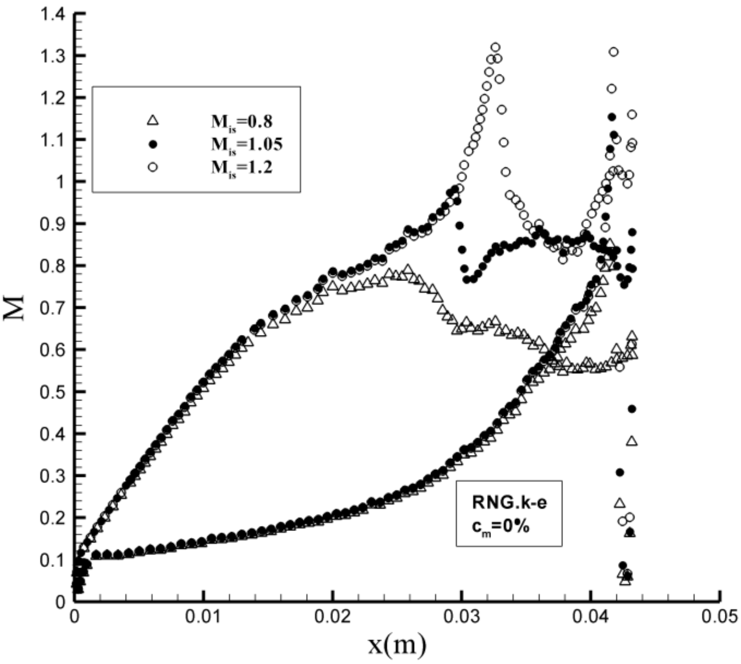

Figure 8 The Mach number distribution on the TE blades without cooling air (C_m = 0%) at Mach 0.8, 1.05 and 1.2 using turbulence modeling of RNG.k-ε

To validate the results, the results of theoretical research with experimental results by Michael Julie [5] for Mach number 1.2 have been compared in Figure (9). Accuracy and validity of the current work compared to experimental work is shown in this figure.

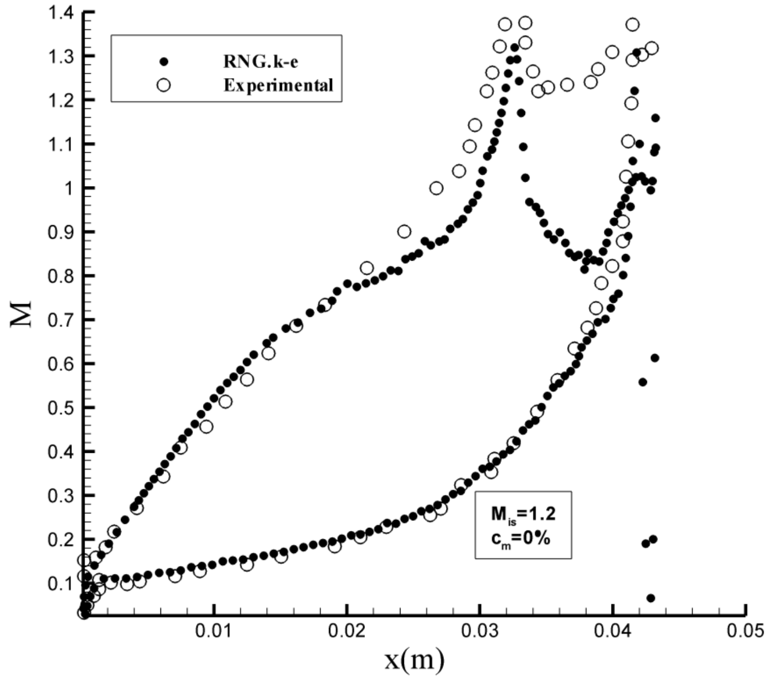

Figure 9 The Mach number distribution on the TE blades without cooling air (C_m = 0%) at Mach 1.2 using turbulence modeling of RNG.k-ε and experimental results

The next step was the cooling air flowing effect from slot on the Mach number distribution of the blade surface. The results obtained at the outlet isentropic Mach number values of 0.8, 1.05, and 1.2 with C_m=3% are shown in Figures (10) to (12). Comparison of the present study's results showed the effectiveness of RNG.K-ε and RSM models for the case of the cooling air through the trailing edge. In these results, it was noticed that the Mach number was decreased at the trailing edge. However, using cooling air flow through the blade trailing edge caused vortices to be mixed at the blade end. This kind of behavior decreased the Mach number loss. These results can be obtained from the presented figures. The Mach number was decreased more at the throat. Comparison of the Mach number decrease was also shown for the cases C_m=0% and C_m=3% and happened at the outlet isentropic Mach numbers of 1.05 and 1.2.

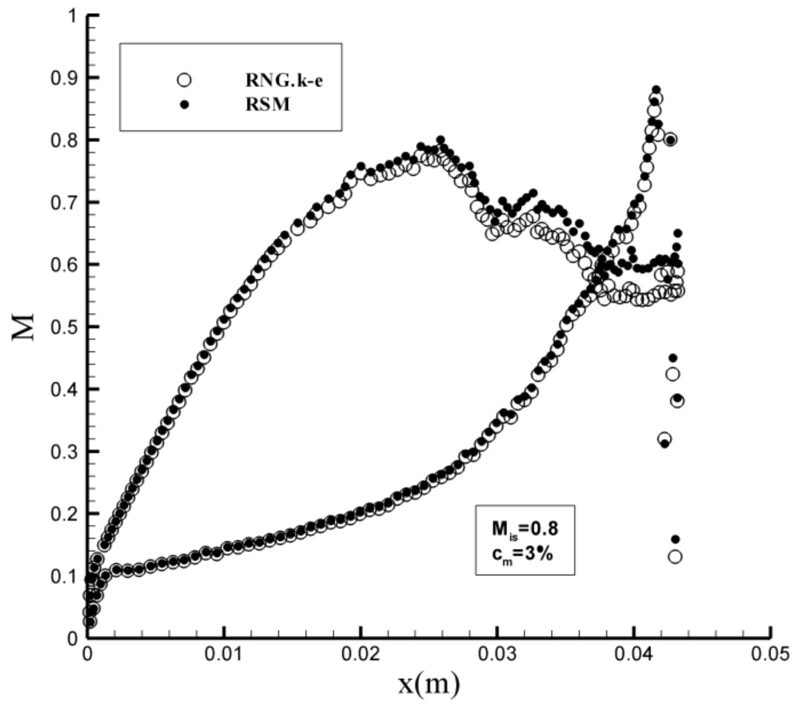

Figure 10 The Mach number distribution on the TE blades with cooling air (C_m = 3%) at Mach 0.8 using turbulence modeling of RNG.k-ε and RSM

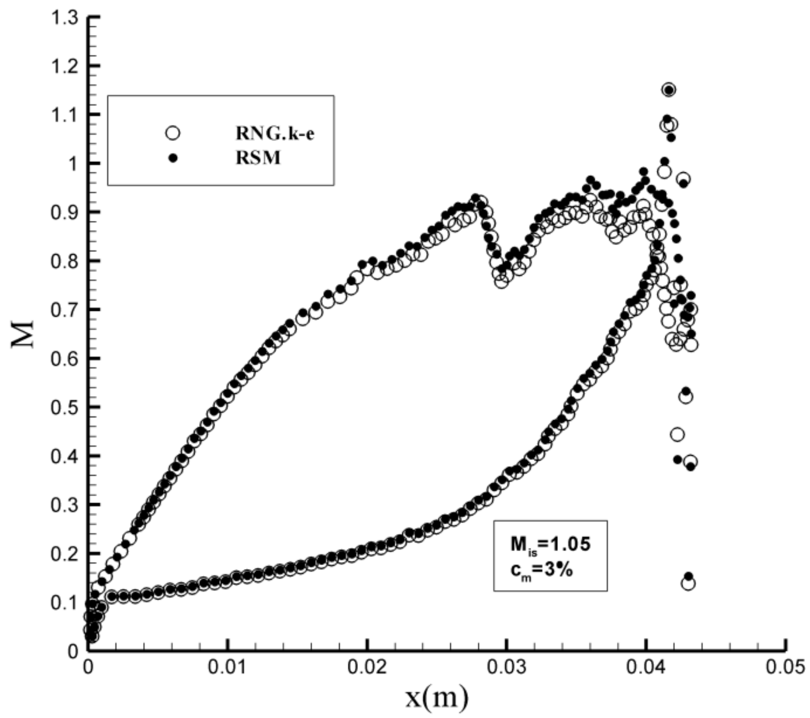

Figure 11 The Mach number distribution on the TE blades with cooling air (C_m = 3%) at Mach 1.05 using turbulence modeling of RNG.k-ε and RSM

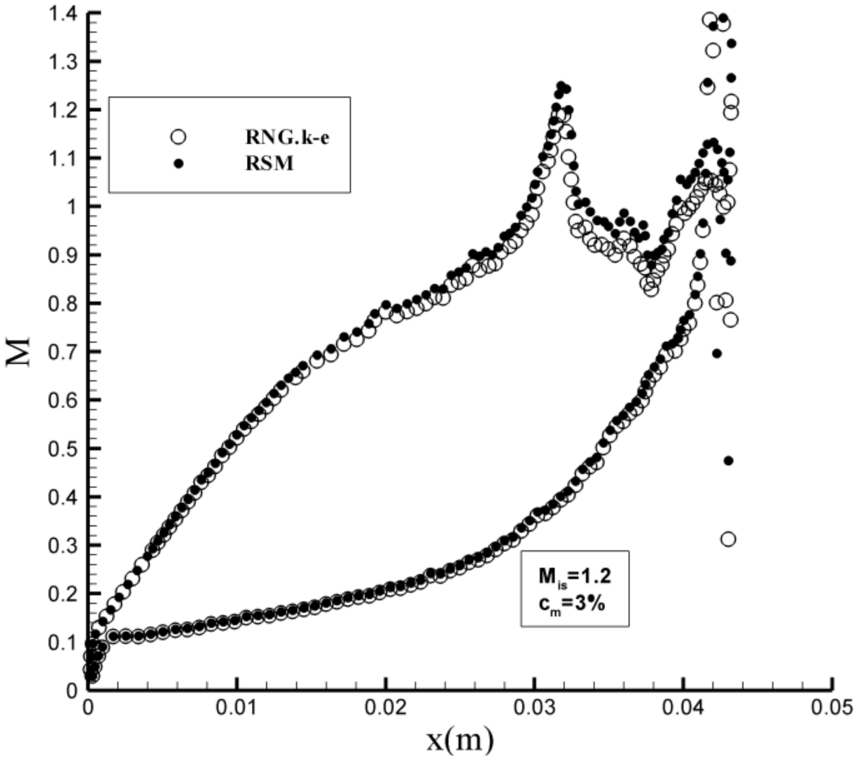

Figure 12 The Mach number distribution on the TE blades with cooling air (C_m = 3%) at Mach 1.2 using turbulence modeling of RNG.k-ε and RSM

Figures (12) and (13) present the surface Mach number distribution for TE blade without cooling air (C_m = 0%) and with cooling air (C_m = 3%) for the outlet isentropic Mach number of 1.05 using RNG.K-ε turbulence model for three different mesh. These results show that the Mach number distribution diagram of mesh of 106314 cells to the next (smaller), the results are fixed and do not change which is independent of the mesh cells show for this amount.

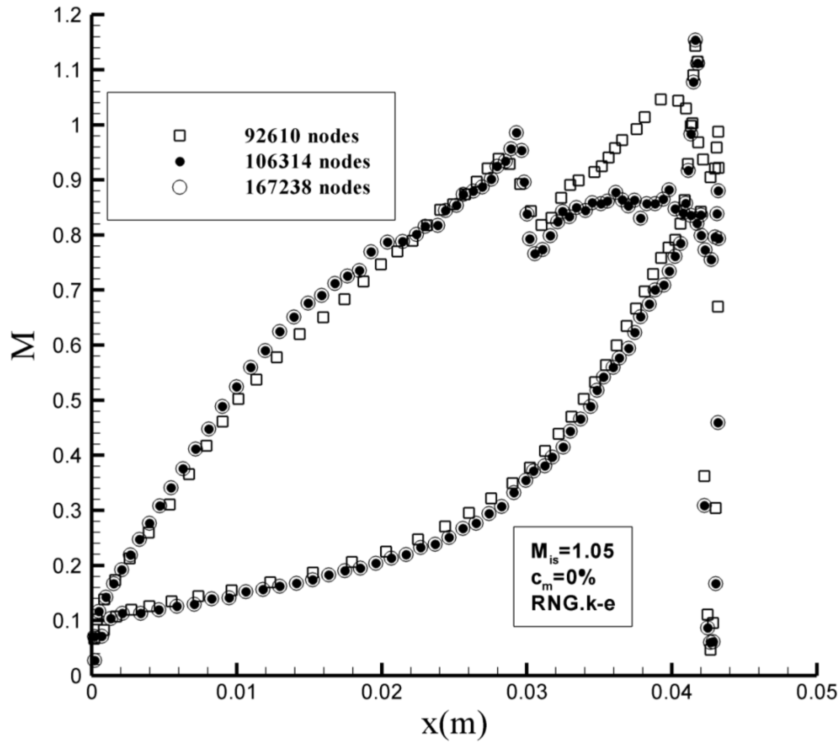

Figure 13 Independent of the mesh for the Mach number distribution on the TE blades without cooling air (C_m = 0%) at Mach 1.05 using turbulence modeling of RNG.k-ε

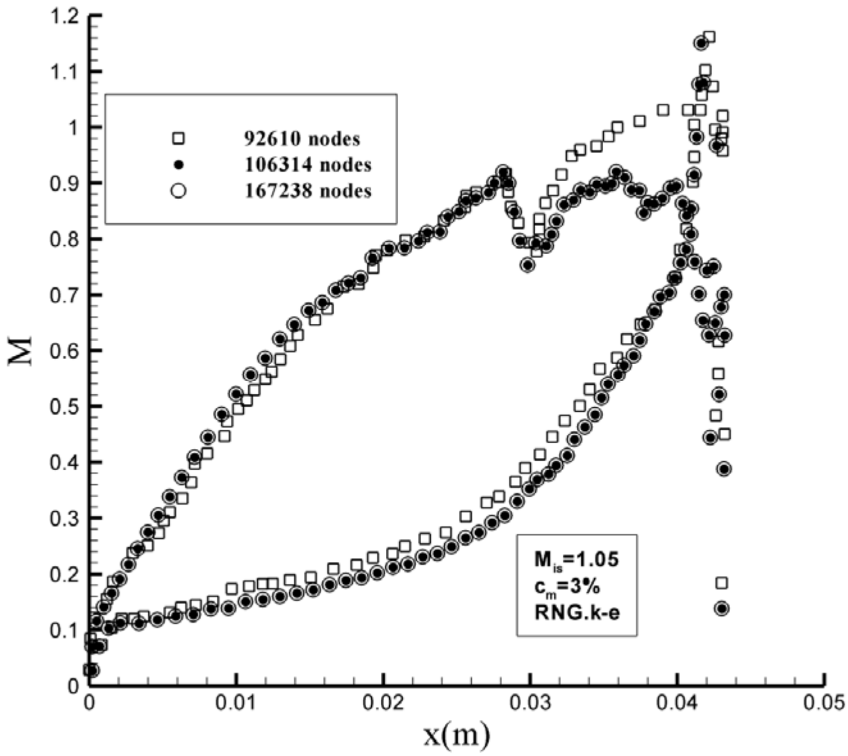

Figure 14 Independent of the mesh for the Mach number distribution on the TE blades with cooling air (C_m = 3%) at Mach 1.05 using turbulence modeling of RNG.k-ε

For the three-dimensional analysis, both cases of without cooling air injection (C_m=0%) and (C_m=3%) and with injection were calculated at the outlet isentropic Mach number 1.05. The Mach number distribution was presented using RNG.K-ε model. The results demonstrated that the three-dimensional solution had great similarity to the two-dimensional analysis. In this case, also, the cooling air flow from the trailing edge caused the Mach number to be decreased. The Mach number at the blade throat decreased when the cooling air was injected. Figures (15) and (16) show that the three-dimensional results had good agreement with the two-dimensional case. It can be claimed that the flow was actually three-dimensional. However, the discussion for being two or three dimensional flow was mostly related to the importance of the dimensions. Consider a flow in which variation in a direction is relatively smaller than another direction. In this case, the behavior of that direction can be neglected and the problem is analyzed using one less space dimension. In a gas turbine blade, those directions that have curvature cannot be invaluable, since the main variation happens in those directions. The blade height in between the other directions has less importance. However, if a blade is twisted or ratio of the radius of tip to root is more than 0.8, in this case, the height direction must be included in the calculation. Most of the old flow analysis and even well-established present computer codes consider two-dimensional analysis and then the third dimension is injected into the calculation by some special techniques. The reason for this procedure is the limited capability of computers in using high mesh numbers during full flow solution. In the present study, the ratio of tip to root radius of blade was small; so, effect of the third dimension was neglected. In the third dimension, the Mach number distribution was similar than the two-dimensional cases; in fact, a three-dimensional case was piled up from many two-dimensional plates.

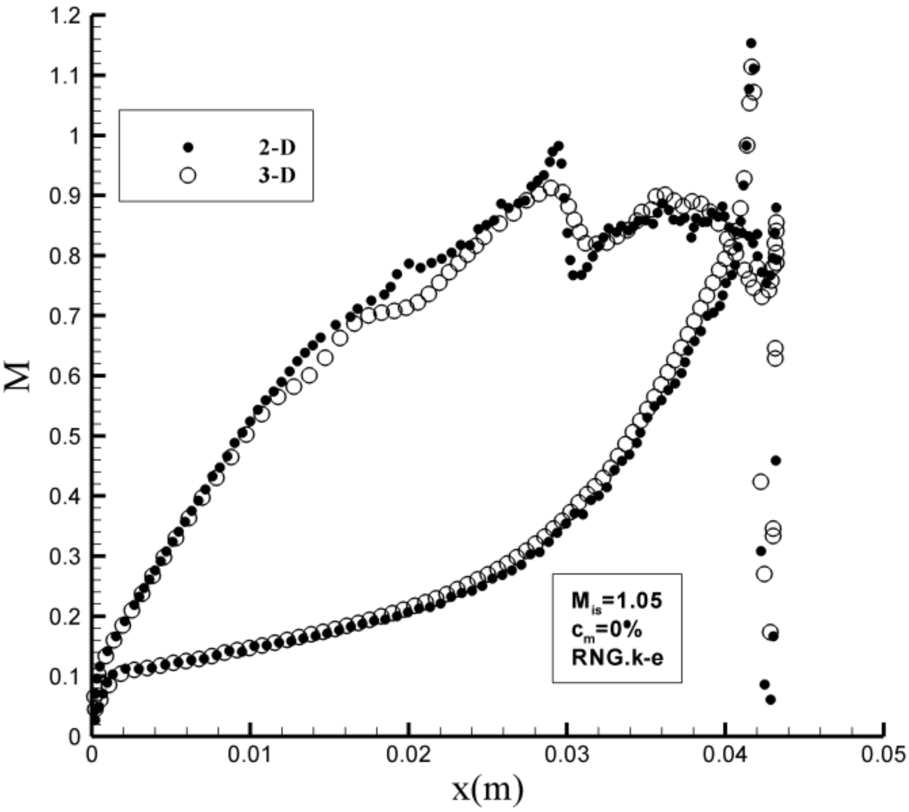

Figure 15 The Mach number distribution on the TE blades without cooling air (C_m = 0%) at Mach 1.05 using turbulence modeling of RNG.k-ε in two and three-dimensional case

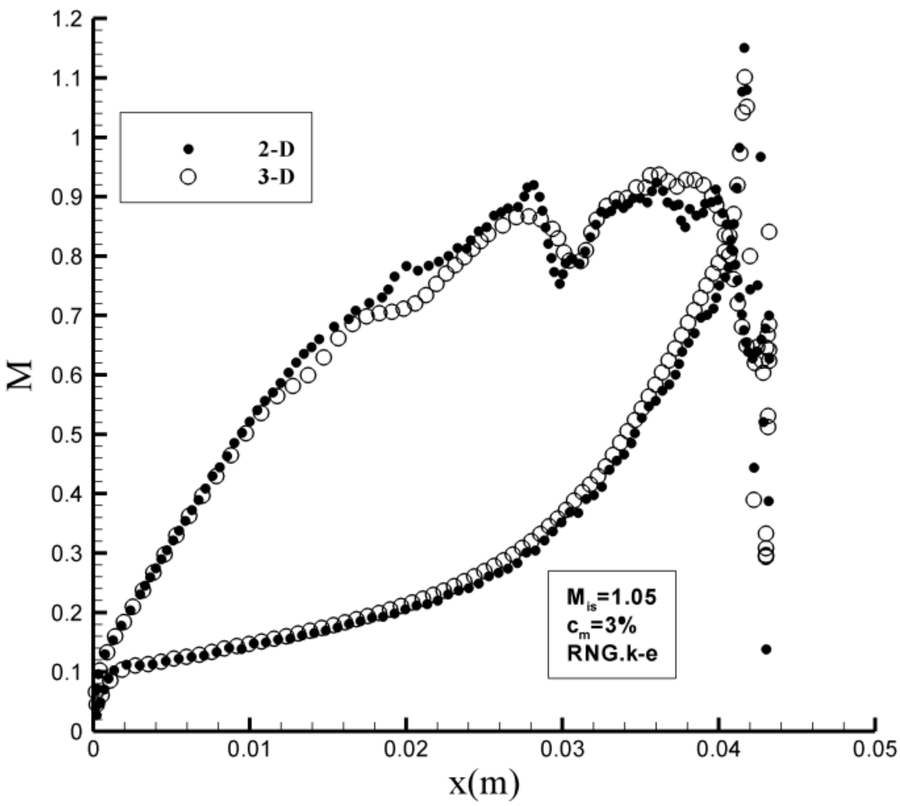

Figure 16 The Mach number distribution on the TE blades with cooling air (C_m = 3%) at Mach 1.05 using turbulence modeling of RNG.k-ε in two and three-dimensional cases

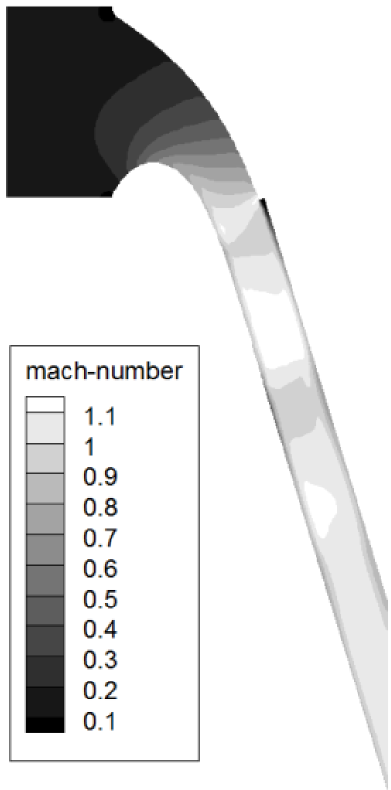

Figure 17 The Mach number contours on the TE blades without cooling air (C_m = 0%) at Mach 1.05 using turbulence modeling of RNG.k-ε

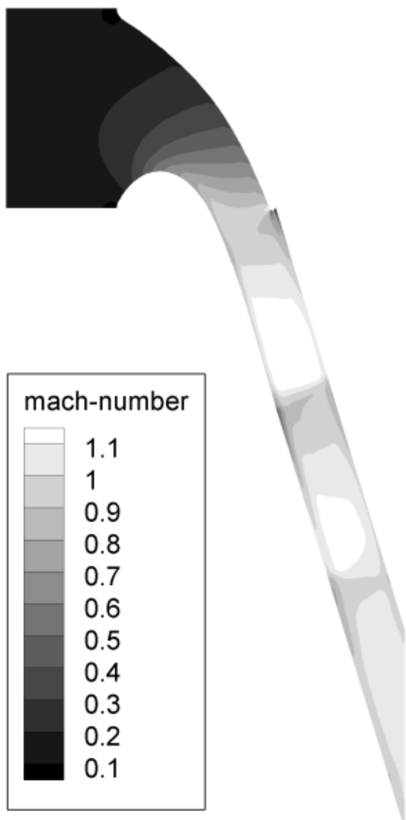

Figure 18 The Mach number contours on the TE blades with cooling air (C_m = 3%) at Mach 1.05 using turbulence modeling of RNG.k-ε

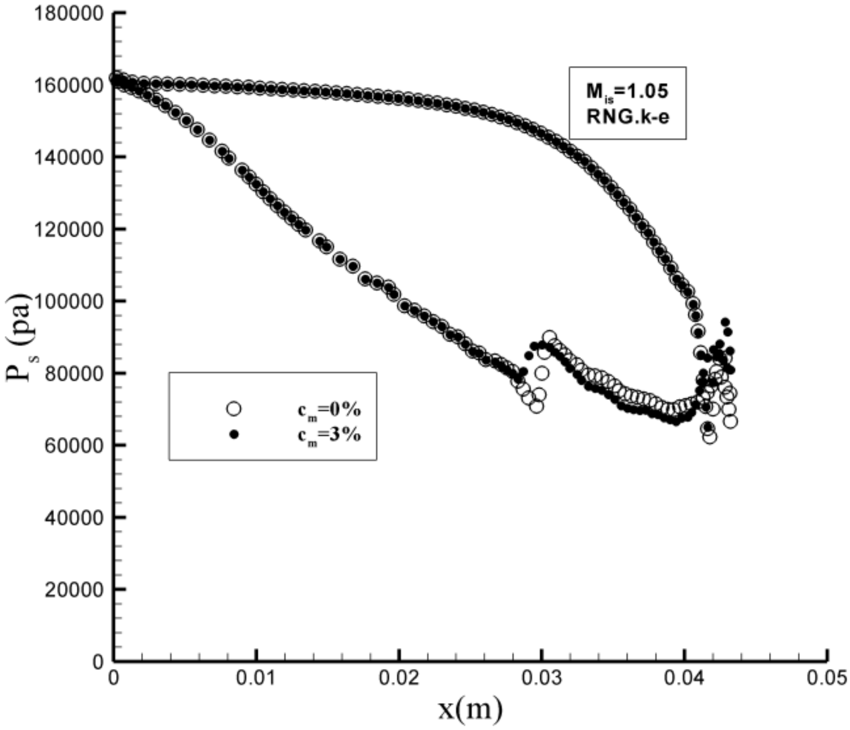

Figure 19 The Static Pressure distribution on the TE blades with and without cooling air (C_m = 0&3%) at Mach 1.05 using turbulence modeling of RNG.k-ε

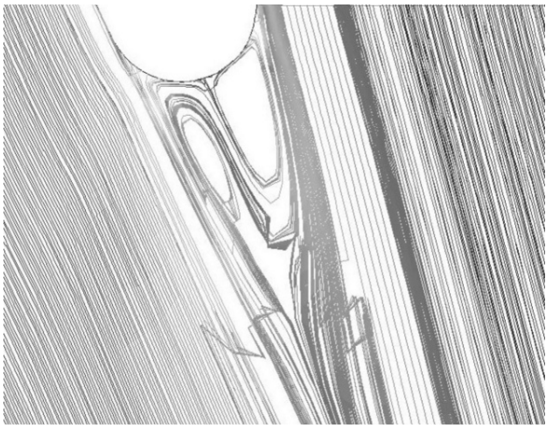

Figure 20 Generated vortices at the trailing edge of the TE blades

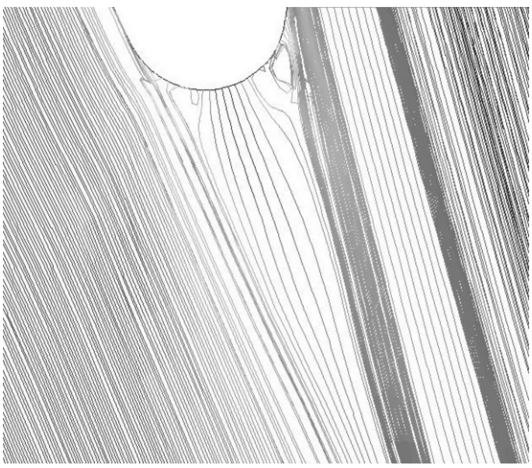

Figure 21 Effects of air injection from the trailing edge of the TE blades on generated vortices

6 Conclusion

Flow field around the TE type of blade was modeled using the full Navier-Stokes equation with high accuracy, as shown in Figures (6) and (17). It can be concluded that:
- The trailing edge curvature at the TE type of blade created vortices, which caused the Mach number to decrease at the end of the blade. The experimental equipment had no capability in measuring this effect (see Figure 19).
- Turbulence modeling of RNG.k-ε and RSM had similar results on the Mach number distribution (see Figures 5, 6, and 7).
- Flow injection of cooling air from the trailing edge caused the generated vortices to be highly eliminated (see Figure 19, 20, and 21).

References

[1] Dunham, J., and Came, P.M., "Improvements to the Ainley-Mathieson Method of Turbine Performance Prediction", Transaction of the ASME, J. Eng. for Power, Ser. A, Vol. 92, pp. 252-256, (1970).

[2] Pritchard, L.J., "An Eleven Parameter Axial Turbine Airfoil Geometry Model", ASME 85- GT-219, Tech. Report, (1985).

[3] Leonard, D., and Van Den Braembussche, R.A., "Inverse Design of Compressor and Turbine Blades at Transonic Flow Condition", the ASME Int. Gas Turbine and Aeroengine Congress and Exhibition, Cologne, Germany, ASME–92- GT-430, (1992).

[4] Denton, J.D., "An Improved Time-marching Method for Turbo Machinery Flow Calculation", ASME J. Eng. for Power, Vol. 105, pp. 514- 524, (1983).

[5] Joly, M., Verstraete, T., and Paniagua, G., "Differential Evolution based Soft Optimization to Attenuate Vane–rotor Shock Interaction in High-pressure Turbines", Applied Soft Computing, Vol. 13, pp. 1882–1891, (2013).

[6] Aminossadati, S. M., and Mee, D. J., "An Experimental Study on Aerodynamic Performance of Turbine Nozzle Guide Vanes with Trailing-edge Span-wise Ejection", ASME, Journal of Turbo Machinery, Vol. 135, pp. 031002.1–2, (2013).

[7] Barigozzi, G., Ravelli, S., Armellini, A., Mucignat, C., and Casarsa, L., "Effects of Injection Conditions and Mach Number on Unsteadiness Arising within Coolant Jets over a Pressure Side Vane Surface", International Journal of Heat and Mass Transfer, Vol. 67, pp. 1220–1230, (2013).

[8] Uzol, O., and Camci, C., "Aerodynamic Loss Characteristics of a Turbine Blade with Trailing Edge Coolant Ejection: Part2-External Aerodynamics, Total Pressure Losses, and Predictions", ASME, Journal of Turbo Machinery, Vol. 132, No. 2, pp. 249-257, (2001).

[9] El-Gendi, M., Lee, K. and Lee, S., "Comparison between Steady and Unsteady Flow Predictions through High Pressure Turbine Cascade", KSME-JSME Thermal and Fluids Engineering Conference, GSF26-020, (2013).

[10] Horbach, T., Schulz, A., and Bauer, H., "Trailing Edge Film Cooling of Gas Turbine Airfoils-effects of Ejection Lip Geometry on Film Cooling Effectiveness and Heat Transfer", Int. Symp. on Heat Transfer in Gas Turbine Systems, Antalya, Turkey, (2009).

[11] Ligrani, Ph., "Aerodynamic Losses in Turbines with and without Film Cooling, as Influenced by Mainstream Turbulence, Surface Roughness, Airfoil Shape, and Mach Number", Hindawi Publishing Corporation, International Journal of Rotating Machinery, Article ID 957421, 28 pages, Vol. (2012).

[12] Patankar, S.V., "*Numerical Heat Transfer and Fluid Flow*", Emisphere Publishing Corporation, London, pp. 214-214, (1980).

[13] Choudhury, D., "Introduction to the Renormalization Group Method and Turbulence Modeling", Tech. Memorandum, Fluent Incorporated, TM-107, pp. 70, (1993).

[14] Saniei Nejad, M., "Comprehensive Investigation of k-ε and k-ω Turbulence Models in Simulation Turbulent Supersonic Boundary Layer Generated over Smooth and Rough Flat Plates at Very High Reynolds Numbers", Journal of Fluid Mechanics and Aerodynamics, Vol. 1, No. 2, pp. 55-72, (2013). (In Persian)

[15] Launder, B.E., Reece, G.J., and Rodi, W., "Progress in the Development of a Reynolds Stress Turbulence Closure", Journal of Fluid Mechanics, Vol. 68, pp. 537–566, (1975).

Nomenclature

D_H	Hydraulic diameter [m]
D_{ij}	Transport by diffusion
G_b	Turbulent kinetic energy production
K	Turbulent kinetic energy [$(m/s)^2$]
K	Thermal conductivity [W/mk]
L	Flow length scale
M	*Mach number*
$\dot{m}$	*Mass flow rate* [kg/s]
Prt	Turbulent Prandtl number
R	Gas constant [J/(kgK)]
R_{ij}	Rate of change
S	Strain rate [1/s]
S_{ij}	Strain rate tensor
Tu , I	Turbulence intensity [%]
u	Local velocity [m/s]
u'	Oscillatory component of velocity [m/s]
v	velocity component parallel to the gravity
x,y,z	Cartesian coordinate system
x_i	i-th coordinates Cartesian coordinate system
y	Distance from the nearest wall [m]
Y_M	Variation of expansion in the compressible turbulence due to the loss rate

Greek symbols

α	*Angle* [°]
μ	Molecular viscosity [Pas]
μ_t	Turbulence viscosity
μ_τ	Shear velocity
ρ	Density [kg/m^3]
τ	Wall shear stress [pa]
τ_{ij}	Deviatoric tensor
ε	Dissipation of turbulence energy rate
ε_{ij}	Rate of dissipation
α_k	effects of Prandtl reverse for k
α_ε	effects of Prandtl reverse for ε
ω	Turbulence frequency [1/s]
ω_k	Rotation vector
Π_{ij}	Transport due to turbulent pressure-strain interactions

Subscripts

i	Direction x_i
j	Direction x_j
b	Under the influence of Buoyancy
k	Under the influence of the mean velocity gradient, Turbulent kinetic energy
ω	In Turbulence frequency

چکیده

در این تحقیق، یک ردیف پره توربین گاز مورد بررسی قرار گرفته است. تجزیه و تحلیل جریان در اطراف پره با استفاده از مدل های آشفتگی RSM و RNG.K-ε و شبیه سازی توسط نرم افزار فلوئنت انجام شده است. نتایج برای مواردی که افت عدد ماخ در لبه فرار پره موجب ایجاد گردابه در انتهای پره می شود، در نظر گرفته شده است. اثر تزریق هوای خنک کننده از لبه فرار پره بر توزیع عدد ماخ در سطح آن موردمطالعه قرار گرفته است. نتایج نشان می دهند که نتایج برای دو مدل آشفتگی RSM و RNG.K-ε مطابقت خوبی داشته و قابلیت مدل اعمالی، توان کافی برای تجزیه و تحلیل رفتار جریان پیچیده را دارد. بر اساس نتایج به دست آمده حاصل از توزیع عدد ماخ بر روی سطح پره، تزریق هوا موجب کاهش افت جریان در لبه فرار آن شده است. مقایسه نتایج به دست آمده نشان می دهند که تزریق هوا به میزان ۳ درصد هوای کل ورودی به ردیف پره باعث تغییرات محل شوک بر روی سطح پره و کاهش افت به میزان ۰/۷ درصد در پره توربین شده است.